The Journal of Antibiotics (2014) 67, 519–525

www.nature.com/ja

ORIGINAL ARTICLE

New myxothiazols from the predatory bacterium *Myxococcus fulvus*

Sebastian Schieferdecker[1], Thomas E Exner[2], Harald Gross[3,4], Martin Roth[5] and Markus Nett[1]

Extracts of the predatory bacterium *Myxococcus fulvus* HKI 722 showed promising antimicrobial activities in the agar diffusion assay. A combined chemical and computational analysis led to the identification of five thiazole-containing antibiotics. Two of the isolated compounds represent previously unrecognized members of the myxothiazol family of natural products. Their antibiotic properties were determined in comparison with those of the known myxothiazols A and Z.
The Journal of Antibiotics (2014) **67,** 519–525; doi:10.1038/ja.2014.31; published online 2 April 2014

Keywords: antibiotic; *Myxococcus fulvus*; myxothiazol; predatory bacteria

INTRODUCTION

Antibiotics are one of the pillars of modern medicine. The misuse of these drugs for prophylactic purposes or for enhancing the growth of livestock is known to exert a selection pressure on microbial communities, which ultimately favors the spread of resistant organisms. Due to the irrational application of antibiotics, the number of pathogens that do not respond to first-line therapeutics steadily increases. This, in turn, urges the need for the discovery of novel drugs, especially for the treatment of nosocomial infections.[1]

Due to their structural diversity and high affinity to biological targets, natural products are ideal lead structures for drug development. Predatory bacteria can be considered as a promising and largely untapped resource to identify new antibiotics.[2] Recent evidence suggests that secondary metabolites of predatory bacteria contribute to their feeding strategy by killing or paralyzing prey organisms.[3,4] Furthermore, it is conceivable that compounds, which mediate cell lysis, can also be used to facilitate the digestion and consumption of prey. Myxobacteria are particularly noteworthy in the context of drug discovery, as single strains possess the genomic potential to produce a huge diversity of natural products.[5,6] Many of the encoded compounds feature unique structural scaffolds and exhibit rare modes of action.[7]

Here, we report the isolation and taxonomic identification of the predatory, myxobacterial strain HKI 722 as well as the bioactivity-guided isolation of five antimicrobial compounds. Two of the metabolites (**1**, **2**) were identified as new myxothiazol derivatives (Figure 1), whereas the remaining compounds represent previously described members of this natural product family, including myxothiazol A (**3**), myxothiazol Z (**4**) and desmethylmyxothiazol (**5**).

RESULTS

Isolation and taxonomy of the producing strain

Strain HKI 722 was isolated in the course of sampling predatory bacteria from the shores of the river Saale, Germany, using a baiting technique. The isolate grew well in the complex medium MD1, but was not able to grow in chemically defined minimal media with glucose as sole carbon source. The growth optimum was observed in the temperature range between 30 °C and 35 °C. On solid media, the bacterium formed red colored swarms. Microscopic analysis revealed non-flagellated vegetative cells, which appeared as slender rods with tapering ends. They exhibited a diameter of 0.5 μm and a length from 3.0 to 10.0 μm. The formation of fruiting bodies, which is a phenotypic hallmark of many myxobacteria,[8] was not observed. Sequencing of the 16S rDNA gene of strain HKI 722 supported a phylogenetic classification as *Myxococcus fulvus* (100% identity with the 16S rDNA gene sequence of *M. fulvus* strain btx2; accession number: KC862605).

Fermentation and isolation procedure for myxothiazols

For the isolation of biologically active compounds, strain HKI 722 was cultured in shaking Erlenmeyer flasks on a 90-l scale. At the end of cultivation, the cells were separated from the fermentation broth by centrifugation. Metabolites that had been secreted into the culture broth during fermentation were recovered with the adsorber resin XAD-2. Following the removal of the supernatant by filtration, the adsorbed compounds were exhaustively eluted from the resin with a 1:1 mixture of methanol and acetone. The resulting extract was concentrated to dryness, resuspended in water and extracted with dichloromethane. The previously observed antimicrobial activity was

[1]Junior Research Group 'Secondary Metabolism of Predatory Bacteria', Leibniz Institute for Natural Product Research and Infection Biology, Hans-Knöll-Institute, Jena, Germany; [2]Pharmaceutical Institute, Department of Pharmaceutical Chemistry, University of Tübingen, Tübingen, Germany; [3]Pharmaceutical Institute, Department of Pharmaceutical Biology, University of Tübingen, Tübingen, Germany; [4]German Centre for Infection Research (DZIF), Partner Site Tübingen, Tübingen, Germany and [5]Bio Pilot Plant, Leibniz Institute for Natural Product Research and Infection Biology, Hans-Knöll-Institute, Jena, Germany
Correspondence: Dr M Nett, Junior Research Group 'Secondary Metabolism of Predatory Bacteria', Leibniz Institute for Natural Product Research and Infection Biology, Hans-Knöll-Institute, Beutenbergstrasse 11a, Jena 07745, Germany.
E-mail: markus.nett@hki-jena.de
Received 7 October 2013; revised 14 February 2014; accepted 5 March 2014; published online 2 April 2014

tracked to the organic phase, which was hence subjected to reversed-phase HPLC, yielding 5.4 mg of myxothiazol S1 (**1**) and 7.8 mg of myxothiazol S2 (**2**). The production of the previously described myxothiazols was considerably larger. Overall, 28.8 mg of **3**, 22.2 mg of **4** and 93.6 mg of **5** were isolated.

Structure determination

The molecular formula of **1** was assigned to be $C_{17}H_{21}N_3O_4S_2$ by high-resolution ESI-MS, which corresponds to nine degrees of unsaturation. An inspection of the ^{13}C NMR spectrum confirmed the deduced number of carbon atoms (Table 1). Furthermore, a total of 10 signals could be ascribed to sp^2-hybridized carbons based on their chemical shifts, including a ketone function resonating at δ_C 207.8 (C-3). The ^1H NMR spectrum of **1** showed 18 non-exchangeable protons. First-order multiplet analysis and homonuclear COSY revealed two independent spin systems, namely a 1-hydroxyethyl residue and a –CH(CH_3)–CH(OR)–CH = CH– partial structure (Figure 2). The latter covered the carbon atoms C-4 to C-7 and C-17. HMBC data allowed the linkage of C-4 with a 2-carbamoylacetyl moiety. H-4, H-5 and H_3-17 showed long-range correlations to C-3. The same carbon atom was also observed by the methylene protons of C-2, which exhibited another specific HMBC to C-1 (δ_C 169.7). An HMBC from H_3-16 to C-5 established the presence of a methoxy group at C-5. The two remaining proton singlets at δ_H 7.17 and 7.99 belonged to sp^2-hybridized methine groups and were

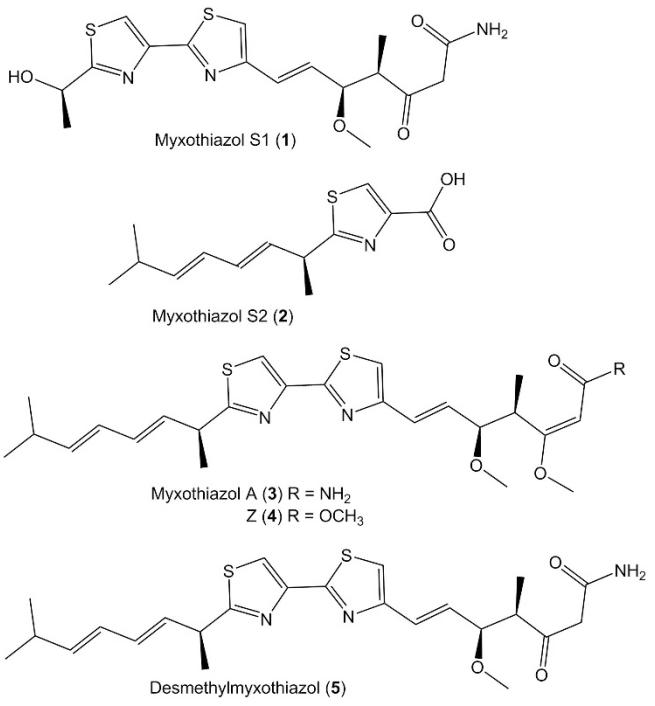

Figure 1 Structures of isolated myxothiazols **1**–**5** from strain HKI 722.

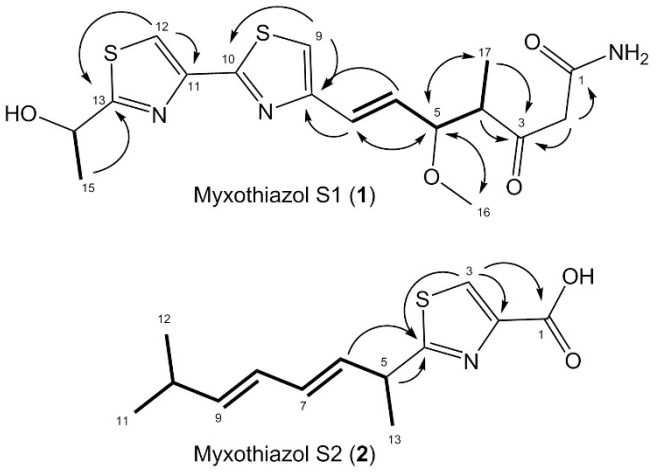

Figure 2 $^1H,^1H$ COSY (bold lines) and selected $^1H,^{13}C$ long-range correlations (arrows) in myxothiazol S1 (**1**) and myxothiazol S2 (**2**).

Table 1 NMR spectroscopic data of 1 in chloroform-d_1

Pos.	δ_H[a]	δ_C[b]	*HMBC*[a] *(H→C)*	*COSY*[a] *(H→H)*	*NOESY*[a] *(H→H)*
1	—	169.7, C_{quat}	—	—	—
2	a 3.65, 1 H (d, 17.8)	48.0, CH_2	1, 3	2b	2 b
	b 3.55, 1 H (d, 17.8)			2a	2 a
3	—	207.8, C_{quat}	—	—	—
4	2.98, 1 H (dq, 5.3, 7.0)	52.0, CH	3	5, 17	5, 17
5	4.02, 1 H (dd, 5.3, 7.7)	82.8, CH	3, 7, 16, 17	4, 6	4, 6, 16
6	6.42, 1 H (dd, 15.7, 7.7)	129.2, CH	8	5, 7	5
7	6.63, 1 H (d, 15.7)	126.7, CH	5, 8	6	—
8	—	153.3, C_{quat}	—	—	—
9	7.17, 1 H (s)	116.6, CH	8, 10	—	—
10	—	162.8, C_{quat}	—	—	—
11	—	148.5, C_{quat}	—	—	—
12	7.99, 1 H (s)	116.8, CH	11, 13	—	—
13	—	176.7, C_{quat}	—	—	—
14	5.20, 1 H (q, 6.5)	68.2, CH	15	15	15
15	1.69, 3 H (d, 6.5)	24.1, CH_3	13, 14	14	14
16	3.33, 3 H (s)	57.0, CH_3	5	—	5
17	1.18, 3 H (d, 7.0)	11.6, CH_3	3, 5, 14	4	4

[a]Recorded at 500 MHz.
[b]Recorded at 125 MHz.

distinguished by large $^{1}J_{CH}$ values (187 Hz in case of CH-9 and 192 Hz in case of CH-12), which places them next to either a nitrogen or a sulfur atom.[9] Both singlets were individually correlated with two quaternary aromatic carbons in the HMBC spectrum. The elemental composition of **1** as well as the observed chemical shifts was consistent with the presence of two thiazole rings.[10–13] HMBCs from H-6 and H-7 to C-8 as well as from H_3-15 to C-13 eventually led to two major fragments that could only be connected *via* C-10 and C-11, thus establishing the planar structure of **1**. To determine the configuration of the carbinol group in **1**, the (*R*)- and (*S*)-Mosher esters were prepared. In case of the methyl protons in position 15, an $\Delta\delta^{SR}$ value of +0.007 p.p.m. was measured indicating the (*R*) configuration.[14] Since the esterification of the secondary alcohol in **1** did not affect the chemical shifts of further protons and the observed chemical shift difference was also rather small, this stereochemical assignment must be considered with care. The relative orientation of H-4 and H-5 was examined by using molecular modeling, $^{3}J_{HH}$ coupling constant analysis and synthetically prepared reference compounds. A combination of molecular mechanics and quantum mechanics calculation was performed on all four remaining stereoisomers of **1** with 4*R*,5*S*,14*R*, 4*S*,5*R*,14*R*, 4*R*,5*R*,14*R* and 4*S*,5*S*,14*R* configurations. In case of the 4*R*,5*R*,14*R* and 4*S*,5*S*,14*R* configuration, all structures within 5 kJ mol^{-1} of the lowest-energy conformer showed with an H_4-C_4-C_5-H_5 torsion angle of ~180° solely an *anti* conformation (III in Figure 3). In contrast, the anti ($\angle H_4$-$H_5 \sim 180°$, III in Figure 3) and one gauche ($\angle H_4$-$H_5 \sim 55°$) H-H arrangement (I and V in Figure 3) have almost the same energy in the 4*R*,5*S*,14*R* and 4*S*,5*R*,14*R* configurations and both arrangements are present in the set of lowest-energy conformations (5 kJ mol^{-1} window from the lowest-energy conformation generated). The dihedral angles acquired from these models were translated into coupling constants, using quantum mechanics calculations on the one hand and by application of the advanced Karplus-type equation proposed by Smith and Barfield[15] on the other hand (Table 2). The experimental $^{3}J_{H4\text{-}H5}$ value (5.3 Hz) almost corresponded to the gauche conformations of the 4*R*,5*S* and 4*S*,5*R* stereoisomers (Table 2) and consequently ruled out all *anti* conformations, whose *J*-values were nearly double the size and ranged from 10 to 11 Hz. The results from the theoretical experiments were verified by analysis of synthetically prepared reference compounds, namely the *syn* (**6**) and the *anti* diastereomers (**8**) of *(E)*-5-hydroxy-4-methyloct-6-en-3-one (Figure 4). Consistent with the computational calculations, we determined for **6** a coupling constant of 4.1 Hz and for **8** a coupling constant of 8.7 Hz. It has to be noted that, according to the literature data, the coupling constants of β-hydroxy-α-methyl ketones and β-methoxy-α-methyl ketones are in good accordance.[16–21] While the α- and β-protons of *anti* diastereomers consistently exhibit *J*-values between 8 and 10 Hz, the corresponding coupling constants in *syn* diastereomers are typically observed between 4 and 6 Hz.[16–21] The $^{3}J_{H4\text{-}H5}$ value of **1** would therefore suggest a *syn* orientation which, again, supports either a 4*R*,5*S* or a 4*S*,5*R* configuration. This result is in agreement with the configuration of compound **3**, whose stereochemistry was determined as 4*R*,5*S* by degradation experiments.[22] Since **1** and **3** likely derive from the same biosynthetic pathway,[23] it is reasonable to assume that both compounds possess the same absolute configuration in positions 4

Table 2 Conformational analysis of 1

14R-Stereoisomers of 1	Φ_{DFT}[a]	J_{calc} *Smith–Barfield equation*	J_{calc} *QM methods*
4*R*,5*S*	−54.7 to −56.1 (V)	4.4–4.6	5.9–6.0
	+176.1 to +179.8 (III)	11.1	10.0–10.3
4*R*,5*R*	+177.8 to +179.5 (III)	11.1	10.0–10.2
4S,5*S*	− 179.4 to −179.6 (III)	11.1	10.2
4S,5*R*	+55.1 to +55.6 (I)	4.4–4.6	6.0
	−175.6 to −176.0 (III)	11.1	10.4

Abbreviations: DFT, density functional theory; QM, quantum mechanics.
Torsion-angle H4-C4-C5-H5 of the minimum conformers within an energy window of 5 kJ mol^{-1} (Φ_{DFT} in deg) and calculated coupling constants ($^{3}J_{H4\text{-}H5}$ in Hz) for the four possible stereoisomers of 14*R*-configurated myxothiazol S1 **1**.
[a]Roman numbers in parentheses refer to the corresponding conformation visualized in Newman projection in Figure 3.

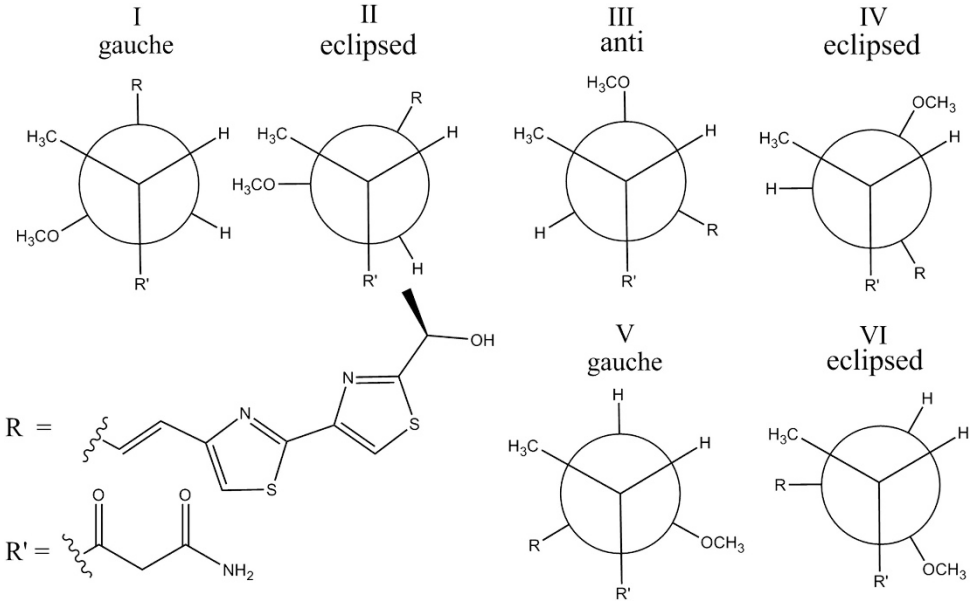

Figure 3 Newman projection of myxothiazol S1 (**1**) along the axis of the C-4/C-5 bond.

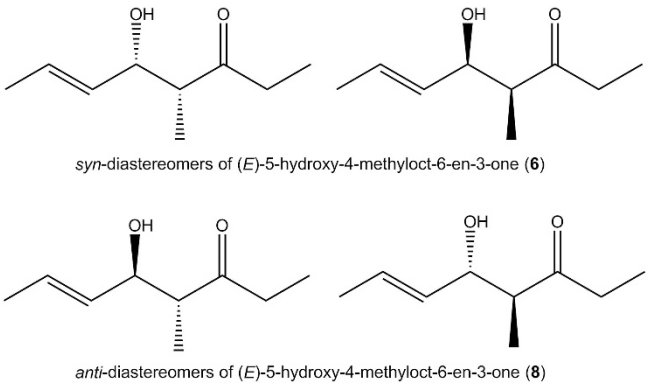

Figure 4 Structures of compounds **6** and **8**.

Table 3 NMR spectroscopic data of 2 in chloroform-d_1

Pos.	δ_H[a]	δ_C[b]	*HMBC*[a] *(H→C)*	*COSY*[a] *(H→H)*
1	—	162.7, C_{quat}	—	—
2	—	145.6, C_{quat}	—	—
3	8.17, 1H (s)	127.8, CH	1, 2, 4	—
4	—	177.0, C_{quat}	—	—
5	3.94, 1H (quint, 7.1)	41.2, CH	4, 6, 7, 13	6, 13
6	5.75, 1H (dd, 15.2, 7.1)	131.7, CH	4, 5, 8, 13	5, 7
7	6.18, 1H (dd, 15.2, 10.3)	132.4, CH	5, 9	6, 8
8	6.01, 1H (dd, 15.3, 10.3)	126.3, CH	6, 10	7, 9
9	5.70, 1H (dd, 15.3, 6.7)	142.9, CH	7, 10, 11, 12	8, 10
10	2.34, 1H (m)	31.1, CH	8, 9, 11, 12	9, 11, 12
11	1.01, 3H (d, 6.7)	22.2, CH_3	9, 10, 12	10
12	1.01, 3H (d, 6.7)	22.2, CH_3	9, 10, 11	10
13	1.54, 3H (d, 7.1)	20.7, CH_3	4, 5, 6	5

[a]Recorded at 500 MHz.
[b]Recorded at 125 MHz.

and 5. Together with the results from the Mosher analysis, we hence propose a 4*R*,5*S*,14*R* configuration for **1**.

For compound **2**, high-resolution ESI-MS gave an exact mass at *m/z* 252.1059 for the $[M+H]^+$ ion, which is consistent with a molecular formula of $C_{13}H_{17}NO_2S$ and corresponds to six degrees of unsaturation. The ^{13}C NMR spectrum exhibited only 12 discrete resonances, but one of the signals showed a very high intensity, suggesting the presence of a magnetically equivalent carbon atom. Except for a singlet resonating at 8.14 p.p.m., all proton NMR signals of **2** were split into multiplets (Table 3). Interpretation of the coupling patterns together with COSY data led to the elucidation of a 1,6-dimethyl-hepta-2*E*,4*E*-dienyl moiety. The two conjugated double bonds are oriented s-*trans*, as evidenced by the vicinal coupling between H-7 and H-8 (*J* 10.3 Hz) and comparison with literature values.[10] It is hence obvious that no steric effects occur that prevent the acyclic diene from achieving a near planar conformation. The remaining resonances were assigned to a thiazole-4-carboxylate unit based upon an analysis of HMBC data and comparison of the observed chemical shifts with literature values.[24] According to HMBCs the thiazole ring was clearly attached to the former fragment (Figure 2), concluding the structure determination. The absolute configuration of compound **2** was not determined experimentally. For biosynthetic reasoning, the same stereochemistry as in compound **3** is proposed. The isolated compounds **3–5** were identified as myxothiazol A, myxothiazol Z and desmethylmyxothiazol, respectively, after comparison of their spectroscopic data with literature values.[10,13,25,26]

Table 4 Antimicrobial activities of the isolated myxothiazols 1–5

Compounds	*Bacillus subtilis*	*Mycobacterium vaccae*	*Pseudomonas aeruginosa*	*Sporobolomyces salmonicolor*	*Penicillium notatum*
1	10	n.a.	12	n.a.	n.a.
2	10	n.a.	12	11	n.a.
3	n.a.	12	n.a.	20	20
4	12	17	n.a.	19	19
5	13	17	n.a.	10	10
Ciprofloxacin	30	24	30	n.d.	n.d.
Amphotericin B	n.d.	n.d.	n.d.	19	18

Abbreviations: n.a., no activity observed; n.d., activity not determined.
The given values represent the diameters of the respective inhibition zone in the agar diffusion assay.

Antimicrobial activities

The purified compounds **1–5** were profiled in the agar diffusion assay against bacteria and fungi that are likely to be encountered in the natural environment of the soil inhabiting *M. fulvus* (Table 4). Except for **3**, all myxothiazols were active against *Bacillus subtilis*. The compounds **1** and **2** also inhibited the growth of *Pseudomonas aeruginosa*, but lacked activity against the actinomycete *Mycobacterium vaccae*. The opposite antibacterial profile was observed for the known metabolites **3–5**. Furthermore, **3** and **4** possessed strong antifungal properties against *Sporobolomyces salmonicolor* and *Penicillium notatum*. The observed zones of inhibition were comparable to that of the reference compound amphotericin B. In contrast, the compounds **1**, **2** and **5** exhibited negligible or no antifungal activity.

DISCUSSION

The myxothiazols are thiazole-containing natural products, which are produced by different species within the myxobacterial family Cystobacteraceae.[10–12] In this study, we confirmed that the soil-derived *M. fulvus* strain HKI 722 is capable to produce a small series of myxothiazol derivatives with complementing antimicrobial activities. Two of the isolated compounds, myxothiazol A (**3**) and Z (**4**), had previously been demonstrated to possess significant antifungal properties due to an inhibition of the cytochrome bc_1 complex of the respiratory chain. This activity could be linked to their β-methoxyacrylate residues.[27,28] As expected, no comparable potency was observed for the new analogs myxothiazol S1 (**1**), myxothiazol S2 (**2**) or for the known desmethylmyxothiazol (**5**), because these metabolites lack the aforementioned pharmacophore. Instead **1** and **2** were active against *P. aeruginosa*, whose growth was not affected by any of the other myxothiazols. The arsenal of compounds, which is secreted by strain HKI 722, enables the bacterium to attack a variety of microorganisms that are present in its natural habitat. Whether the isolated myxothiazols are important for predation is currently under investigation.

MATERIALS AND METHODS

General experimental procedures

UV spectra were recorded on a Varian UV–visible Cary spectrophotometer. IR spectra were recorded on an IFS-55 spectrometer (Bruker, Karlsruhe, Germany). Optical rotation was measured using a 0.5-dm cuvette with a P-1020 polarimeter (JASCO, Tokyo, Japan) at 25 °C. High-resolution mass determination was carried out using an Exactive Mass Spectrometer (Thermo Scientific, Bremen, Germany). NMR spectra were recorded at 300 K on Avance

III spectrometers (Bruker) with chloroform-d_1 as solvent and internal standard. The solvent signal was referenced to δ_H 7.26 and δ_C 77.0, respectively. Preparative HPLC was conducted on a Shimadzu HPLC system (Shimadzu, Kyoto, Japan) consisting of a LC-20AT pump and a SPD-M20A photodiode array detector.

Isolation of predatory bacteria

The isolation of strain HKI 722 and other predatory bacteria was achieved by a baiting technique. Briefly, 25–50 mg of soil samples was placed on pure water agar (WAT agar: $CaCl_2 \times 2H_2O$ 0.1% (w/v), agar 1.5% (w/v), 3-(N-morpholino)propanesulfonic acid 20 mM, 50 μg ml^{-1} cycloheximide, pH 7.2), which had been spotted with suspensions of living *Escherichia coli* DH5α cells. The plates were then incubated at 30 °C for 5 days. Lysis of the *E. coli* spots during the incubation period indicated the presence of predators. To obtain pure cultures, smears of the lytic zones were transferred to fresh WAT-*E. coli* or VY/2 agar plates (Baker's yeast 0.5% (w/v), $CaCl_2 \times 2\ H_2O$ 0.1% (w/v), vitamin B_{12} 0.000005% (w/v), agar 1.5% (w/v)), respectively. Subsequent cultivations were conducted at 30 °C in Erlenmeyer flasks filled with MD1 broth. MD1 medium consisted of casitone 0.3% (w/v), $CaCl_2 \times 2H_2O$ 0.07% (w/v), $MgSO_4 \times 7H_2O$ 0.2% (w/v), vitamin B_{12} 0.00005% (w/v), 1 ml trace elements solution SL-4 (EDTA 0.05% (w/v), $FeSO_4 \times 7H_2O$ 0.02% (w/v), $ZnSO_4 \times 7H_2O$ 0.001% (w/v), $MnCl_2 \times 4H_2O$ 0.0003% (w/v), H_3BO_3 0.003% (w/v), $CoCl_2 \times 6H_2O$ 0.020% (w/v), $CuCl_2 \times 2H_2O$ 0.0001% (w/v), $NiCl_2 \times 6\ H_2O$ 0.0002% (w/v), $Na_2MoO_4 \times 2H_2O$ 0.0003% (w/v)), pH 7.2.

Isolation of genomic DNA and 16S rDNA analysis

Genomic DNA was isolated from a 3-ml aliquot of a growing MD1 culture using the DNeasy Blood & Tissue Kit (QIAGEN, Valencia, CA, USA). The 16S rDNA gene was amplified from the genomic DNA using the primer pair p1 (5′-GGCGTAAAGCGCGTGTAGGC-3′) and p2 (5′-CAWRSAGTCGAGTTG-CAGA CTB-3′). The reaction (50 μl total volume) included 2 mM $MgSO_4$, 0.2 mM each dNTP, 5% dimethyl sulfoxide, 50 pmol of each primer and 1.25 U Pfu DNA polymerase. Thermal cycling conditions were as follows: initial denaturation, 5 min, 95 °C; amplification, 30 cycles (95 °C for 1 min, 65 °C for 1 min and 72 °C for 1 min); final extension, 20 min, 72 °C. The PCR product was purified by agarose gel electrophoresis and subsequently sequenced.

Fermentation and isolation of secondary metabolites

Large-scale cultivation of strain HKI 722 was carried out in 5-l Erlenmeyer flasks. The flasks were shaken (120 r.p.m.) at 30 °C for 7 days. After cultivation, the cells were separated from the fermentation broth by centrifugation at 11 000 r.p.m. for 10 min. Metabolites that had been secreted into the culture broth during cultivation were recovered by adsorption onto 15 g l^{-1} Amberlite XAD-2 resin (Supelco, Bellefonte, PA, USA) overnight. The resin was separated from the supernatant by filtration, washed with 1 l deionized water and extracted three times with 500 ml of a 1:1 mixture of methanol and acetone. The organic extracts were combined and evaporated to dryness under reduced pressure. The resulting residue was resuspended in 100 ml deionized water and extracted three times with 100 ml dichloromethane. The dichloromethane layers were combined, stirred with 5 g water-free Na_2SO_4, filtrated and dried under reduced pressure. This extract was then chromatographed with a Shimadzu UFLC liquid chromatography system (Shimadzu) equipped with a photodiode array detector and a Nucleodur PFP RP column (250 × 10 mm, 5 μm; Macherey-Nagel, Düren, Germany) and a DAD. The myxothiazols were eluted using a linear gradient of methanol in water + 0.1% trifluoroacetic acid with wavelength monitoring at 220 and 310 nm. Final purification of each compound was achieved on a Nucleodur C18 HTec column (250 × 10 mm, 5 μm, Macherey-Nagel).

Myxothiazol S1 (1). IR (film): 3337, 2927, 1667, 1455, 1365, 1298, 1175, 1106, 1073, 1020, 802 cm^{-1}. UV/Vis λ_{max} (MeOH) nm (log ε): 218 (4.30), 248 (4.30), 313 (4.04). $[\alpha]_D^{25}$ +83.2 (c 0.95, MeOH). HR-ESIMS: *m/z* 396.1051 $[M+H]^+$, calcd 396.1046 for $C_{17}H_{22}N_3O_4S_2$.

Myxothiazol S2 (2). IR (film): 3028, 2924, 1688, 1651, 1454, 1370, 1295, 1173, 1103, 1069, 1017, 799 cm^{-1}. UV/Vis λ_{max} (MeOH) nm (log ε): 234 (4.51). $[\alpha]_D^{25}$ +102.3 (c 0.87, MeOH). HR-ESIMS: *m/z* 252.1059 $[M+H]^+$, calcd 252.1053 for $C_{13}H_{18}NO_2S$.

Synthesis of the *syn* diastereomers of (*E*)-5-hydroxy-4-methyloct-6-en-3-one (6)

A mixture of 2 ml (20 mmol) of borane dimethyl sulfide was dissolved in 12 ml of dry diethyl ether and heated under an argon atmosphere in a water bath to 35 °C. To this solution, 7.4 ml (46 mmol) of (+)-α-pinene was added dropwise and the solution was stirred for 30 min. Following the precipitation of the (+)-α-pinene borane in an ice-water bath, the solvent was evaporated using a dry argon stream. The pinene borane complex was redissolved in 10 ml of dry n-hexane under an argon atmosphere and cooled in an ice bath. To this solution, 1.6 ml (17.6 mmol) of trifluoromethanesulfonic acid was added. The mixture was stirred for 30 min at room temperature. Upon completion of the reaction, the upper phase was removed, mixed with 10 ml of dry dichloromethane and cooled in an acetone dry ice bath (−78 °C). Afterwards, 1 ml (6 mmol) of Hünig's base and 320 μl (3 mmol) of diethylketone were consecutively added under stirring before the mixture was supplemented with 430 μl (6 mmol) of *trans*-crotonaldehyde. The solution was then stirred for 40 min, during which it turned into a viscous white slime. The latter was extracted three times with 20 ml dichloromethane. The organic layers were combined and dried under reduced pressure to give a colorless dull oil, which was suspended in a mixture of 10 ml of methanol and 3 ml of water. To an ice-cooled solution, 4 ml of 30% hydrogen peroxide solution was added and the solution was stirred for 2 h at room temperature. Afterwards, the solution was poured into 30 ml of water, which was extracted three times with dichloromethane. The dichloromethane extracts were combined and concentrated to 20 ml under reduced pressure. This solution was washed with 20 ml of saturated aqueous $NaHCO_3$ solution and with 20 ml of saturated aqueous NaCl solution. The extract was finally dried with sodium sulfate and dried under reduced pressure giving a colorless oil containing the *syn* diastereomers of *(E)*-5-hydroxy-4-methyloct-6-en-3-one (**6**), which was finally purified by reversed-phase HPLC to yield 101 mg (0.65 mmol, 21.7% yield) of **6**.

syn-(E)-5-hydroxy-4-methyloct-6-en-3-one (6). ^{1}H-NMR (600 MHz, chloroform-d_1) δ_H [p.p.m.] (*J* [Hz]) 1.04 (3 H, t, *J* 7.3, H-1), 1.13 (3 H, d, *J* 7.3, H-9), 1.70 (3 H, dd, *J* 6.5, 1.6, H-8), 2.51 (2 H, q, *J* 7.3, H-2), 2.66 (1 H, dq, *J* 7.3, 4.1, H-4), 4.33 (1 H, m, H-5), 5.45 (1 H, ddq, *J* 15.3, 6.6, 1.6, H-6), 5.71 (1 H, ddq, *J* 15.3, 6.5, 1.2, H-7). ^{13}C-NMR (150 MHz, chloroform-d_1) δ_C [p.p.m.] 7.5 (C-1), 11.0 (C-9), 17.7 (C-8), 35.5 (C-2), 50.6 (C-4), 72.8 (C-5), 128.0 (C-7), 130.6 (C-6), 215.8 (C-3).

Synthesis of the *anti* diastereomers of (*E*)-5-hydroxy-4-methyloct-6-en-3-one (8)

A solution of 20 mg (0.14 mmol) of **6** in 20 ml of dry diethyl ether was mixed with 93.5 mg (0.56 mmol) of *p*-nitrobenzoic acid and 146.8 mg (0.56 mmol) of triphenylphosphine under an argon atmosphere. The solution was then cooled in a water-ice bath (10 °C) and 110 μl (0.56 mmol) of diisopropyl azodicarboxylate was added dropwise. After extended stirring (14 h at room temperature and 3 h at 40 °C), the solution was extracted with a saturated $NaHCO_3$ solution. The aqueous phases were pooled and extracted twice with dimethyl ether. Subsequently, the ether solutions were combined and evaporated to give a yellow oil. The purification of the *anti* diastereomers of (*E*)-5-methyl-6-oxooct-2-en-4-yl 4-nitrobenzoate (**7**) *via* reversed-phase HPLC yielded 24.4 mg (0.08 mmol, 57.1% yield) of product. To cleave the *p*-nitrobenzoic ester, 3.2 mg (0.01 mmol) of **7** was hydrolyzed with 4 mg (0.061 mmol) of sodium azide in 2 ml of dry methanol.[29] The *anti* diastereomers of (*E*)-5-hydroxy-4-methyloct-6-en-3-one (**8**) were obtained in a yield of 0.71 mg (0.0068 mmol, 68.0% yield) following purification by reversed-phase HPLC.

anti-(E)-5-methyl-6-oxooct-2-en-4-yl 4-nitrobenzoate (7). ^{1}H-NMR (300 MHz, chloroform-d_1) δ_H [p.p.m.] (*J* [Hz]) 1.02 (3 H, t, *J* 7.3, H-8), 1.12 (3 H, d, *J* 7.2, H-9), 1.74 (3 H, dd, *J* 6.6, 1.6, H −1), 2.54 (2 H, q, *J* 7.3, H-7), 3.02 (1 H, dq, *J* 8.9, 7.2, H-5), 5.42 (1 H, ddq, *J* 15.3, 8.2, 1.6, H-3), 5.64 (1 H, dd, *J* 8.9, 8.2, H-4), 5.96 (1 H, dq, *J* 15.3, 6.6, H-2), 8.13 (2 H, d, *J* 8.9, H-3′), 8.27 (2 H, d, *J* 8.9, H-4′). ^{13}C-NMR (75 MHz, chloroform-d_1) δ_C [p.p.m.] 7.6 (C-8),

13.3 (C-9), 17.9 (C-1), 35.4 (C-7), 49.7 (C-5), 77.9 (C-4), 123.5 (C-4′), 126.2 (C-7), 130.6 (C-3′), 133.3 (C-6), 135.7 (C-2′), 150.5 (C-5′), 163.4 (C-1′), 212.1 (C-6).

anti-(E)-5-hydroxy-4-methyloct-6-en-3-one (8). ^{1}H-NMR (500 MHz, chloroform-d_1) δ_H [p.p.m.] (J [Hz]) 1.06 (3 H, t, J 7.3, H-1), 1.13 (3 H, d, J 7.3, H-9), 1.71 (3 H, dd, J 6.5, 1.6, H-8), 2.55 (2 H, q, J 7.3, H-2), 2.66 (1 H, dq, J 8.7, 7.3, H-4), 4.41 (1 H, m, H-5), 5.46 (1 H, ddq, J 15.3, 6.6, 1.6, H-6), 5.69 (1 H, ddq, J 15.3, 6.5, 1.2, H-7). ^{13}C-NMR (125 MHz, chloroform-d_1) δ_C [p.p.m.] 7.5 (C-1), 11.1 (C-9), 17.7 (C-8), 35.4 (C-2), 50.6 (C-4), 72.8 (C-5), 128.0 (C-7), 130.6 (C-6), 215.7 (C-3).

Preparation of Mosher esters of 1

To a solution of 1 mg (2.5 µmol) of **1** in 100 µl of dry deuterated chloroform, 1 µl of dry pyridine was added under an argon atmosphere. To this solution, 1 µl of (*R*)- or (*S*)-α-methoxy-α-(trifluoromethyl)phenylacetyl chloride (MTPA-Cl; Sigma-Aldrich, Steinheim, Germany) was added and the solution was shaken at room temperature for 1 h. After incubation, the solutions were directly analyzed by ^{1}H NMR spectroscopy.

Molecular modeling and Karplus calculations

Structures of myxothiazol S1 (**1**) in the 4*R*,5*R*,14*R*, 4*S*,5*S*,14*R*, 4*R*,5*S*,14*R*, as well as 4*S*,5*R*,14*R* configuration were manually generated using the Molecular Operating Environment (MOE) 2012.10 developed by Chemical Computing Group.[30] The conformational space was then thoroughly explored within the same program using the Merck Molecular Force Field 94 (MMFF94)[31] and the stochastic search method with standard settings. Sets between 500 and 600 low-energy structures were produced, which were then further optimized using density functional theory within the Gaussian 09 program package.[32] The B3LYP[33] hybrid functional was combined with the 6–31 g(d,p) basis set.[34–41] Effects of the solvent chloroform were approximated with an implicit solvent model (IEF-PCM)[42–44] based on the self-consistent reaction field. The conformations were ranked according to the sum of electronic and thermal free energy based on normal-mode analysis. All structures within an energy window of 5 kJ mol^{-1} from the lowest-energy conformation were chosen for the calculation of chemical shieldings and coupling constants. The valence triple-ζ basis set 6–311 + g(d,p)[45–48] was used in these calculations. After additional energy optimization with the larger basis set, the NMR parameters were calculated with the GIAO (gauge invariant/including atomic orbitals) formalism[49–51] and the two-step approach for the coupling constants developed by Deng *et al.*[52]

Empirical calculation of the coupling constants $^{3}J_{H4\text{-}H5}$ from the corresponding dihedral angles was performed with MestRe-J,[53] using the Smith-Barfield equation[15] parameterized with the corresponding substituents.

Agar diffusion assay

Antimicrobial activities of **1–5** were determined in a primary screen against *B. subtilis* ATCC 6633, *P. aeruginosa* K799/61, *M. vaccae* IMET 10670, *S. salmonicolor* SBUG 549 and *P. notatum* JP 36. To this end, holes with 7 mm diameter were aseptically punched in the respective agar medium. Subsequently, the agar plates were inoculated with the test organisms. In all, 1 mg of every test compound was dissolved in 1 ml of methanol, and 50 µl of this solution was transferred to a single hole. Ciprofloxacin, amphotericin B and methanol served as positive and negative controls, respectively. After evaporation of the solvent, the agar plates were incubated depending on the growth conditions of the test organisms. A noticeable antimicrobial activity resulted in an inhibition zone of >10 mm.

ACKNOWLEDGEMENTS

We gratefully acknowledge financial support by the DFG-funded graduate school JSMC as well as by the Leibniz Association. We thank A Perner (Hans-Knöll-Institute Jena, Department of Biomolecular Chemistry) for recording HR-ESI-MS spectra and C Weigel (Hans-Knöll-Institute Jena, Department of Molecular and Applied Microbiology) for conducting the agar diffusion assay. We thank the Baden-Württemberg grid (bwGRiD) for providing the computer resources, which enabled the conducted computational calculations.

1 Fischbach, M. A. & Walsh, C. T. Antibiotics for emerging pathogens. *Science* **325,** 1089–1093 (2009).
2 Cain, C. C. *et al.* Synergistic antimicrobial activity of metabolites produced by a nonobligate bacterial predator. *Antimicrob. Agents Chemother.* **47,** 2113–2117 (2003).
3 Volz, C., Kegler, C. & Müller, R. Enhancer binding proteins act as hetero-oligomers and link secondary metabolite production to myxococcal development, motility, and predation. *Chem. Biol.* **19,** 1447–1459 (2012).
4 Xiao, Y., Wei, X., Ebright, R. & Wall, D. Antibiotic production by myxobacteria plays a role in predation. *J. Bacteriol.* **193,** 4626–4633 (2011).
5 Wenzel, S. C. & Müller, R. The impact of genomics on the exploitation of the myxobacterial secondary metabolome. *Nat. Prod. Rep.* **26,** 1385–1407 (2009).
6 Nett, M. & König, G. M. The chemistry of gliding bacteria. *Nat. Prod. Rep.* **24,** 1245–1261 (2007).
7 Weissman, K. J. & Müller, R. Myxobacterial secondary metabolites: bioactivities and modes-of-action. *Nat. Prod. Rep.* **27,** 1276–1295 (2010).
8 Shimkets, L. J., Dworkin, M. & Reichenbach, H. The myxobacteria. in *The Prokaryotes* (eds Dworkin, M., Falkow, S., Rosenberg, E., Schleifer, K.-H. & Stackebrandt, E.) 31–115 (Springer, New York, 2006).
9 Pretsch, E. *Structure Determination of Organic Compounds: Tables of Spectral Data* (Springer, Berlin, Heidelberg, 2009).
10 Trowitzsch, W., Reifenstahl, G., Wray, V. & Gerth, K. Myxothiazol, an antibiotic from *Myxococcus fulvus* (myxobacterales). II. Structure elucidation. *J. Antibiot.* **33,** 1480–1490 (1980).
11 Ojika, M. *et al.* Cystothiazoles A and B, new bithiazole-type antibiotics from the myxobacterium *Cystobacter fuscus*. *J. Antibiot.* **51,** 275–281 (1998).
12 Böhlendorf, B. *et al.* Melithiazols A–N: new antifungal β-methoxyacrylates from myxobacteria. *Eur. J. Org. Chem.* 2601–2608 (1999).
13 Ahn, J. W. *et al.* Bithiazole metabolites from the myxobacterium *Myxococcus fulvus*. *Chem. Pharm. Bull.* **55,** 477–479 (2007).
14 Hoye, T. R., Jeffrey, C. S. & Shao, F. Mosher ester analysis for the determination of absolute configuration of stereogenic (chiral) carbinol carbons. *Nat. Protoc.* **2,** 2451–2458 (2007).
15 Smith, W. B. & Barfield, M. Predictions of ^{3}J(HH) near 180°—reparametrization of the sp^3-sp^3 equation. *Magn. Res. Chem.* **31,** 696–697 (1993).
16 Chow, H.-F. & Seebach, D. Diastereoselective aldol addition using boron trichloride or alkoxydichloroborane. *Helv. Chim. Acta* **69,** 604–614 (1986).
17 Evans, D. A., Nelson, J. V., Vogel, E. & Taber, T. R. Stereoselective aldol condensations via boron enolates. *J. Am. Chem. Soc.* **103,** 3099–3111 (1981).
18 Yoshida, W. Y., Bryan, P. J., Baker, B. J. & McClintock, J. B. Pteroenone: a defensive metabolite of the abducted antarctic pteropod *Clione antarctica*. *J. Org. Chem.* **60,** 780–782 (1995).
19 Gebauer, J., Arseniyadis, S. & Cossy, J. A concise total synthesis of melithiazole C. *Org. Lett.* **9,** 3425–3427 (2007).
20 Horstmann, N. & Menche, D. Configurational assignment of rhizopodin, an actin-binding macrolide from the myxobacterium *Myxococcus stipitatus*. *Chem. Commun.* **2008,** 5173–5175 (2008).
21 Carmeli, S., Moore, R. E. & Patterson, G. M. L. Tolytoxin and new scytophycins from three species of *Scytonema*. *J. Nat. Prod.* **53,** 1533–1542 (1990).
22 Trowitzsch, W., Höfle, G. & Sheldrick, W. S. The stereochemistry of myxothiazol. *Tetrahedron Lett.* **22,** 3829–3832 (1981).
23 Silakowski, B. *et al.* New lessons for combinatorial biosynthesis from myxobacteria. The myxothiazol biosynthetic gene cluster of *Stigmatella aurantiaca* DW4/3-1. *J. Biol. Chem.* **274,** 37391–37399 (1999).
24 Borgen, G. *et al.* Proton magnetic resonance spectra of thiazoles. Chemical shifts and substituent effects. *Acta Chem. Scand.* **20,** 2593–2600 (1966).
25 Ahn, J. W., Woo, S. H., Lee, C. O., Cho, K. Y. & Kim, B. S. KR025, a new cytotoxic compound from *Myxococcus fulvus*. *J. Nat. Prod.* **62,** 495–496 (1999).
26 Steinmetz, H., Forche, E., Reichenbach, H. & Höfle, G. Biosynthesis of myxothiazol Z, the ester-analog of myxothiazol A in *Myxococcus fulvus*. *Tetrahedron* **56,** 1681–1684 (2000).
27 Thierbach, G. & Reichenbach, H. Myxothiazol, a new antibiotic interfering with respiration. *Antimicrob. Agents Chemother.* **19,** 504–507 (1981).
28 Von Jagow, G., Ljungdahl, P. O., Graf, P., Ohnishi, T. & Trumpower, B. L. An inhibitor of mitochondrial respiration which binds to cytochrome b and displaces quinone from the iron-sulfur protein of the cytochrome bc1 complex. *J. Biol. Chem* **259,** 6318–6326 (1984).
29 Gómez-Vidal, J. A., Forrester, M. T. & Silverman, R. B. Mild and selective sodium azide mediated cleavage of *p*-nitrobenzoic esters. *Org. Lett.* **3,** 2477–2479 (2001).
30 Molecular Operating Environment (MOE). (2012.10). 2012. 1010 Sherbooke St West, Suite #910, Montreal, QC, Canada, H3A 2R7, Chemical Computing Group Inc.
31 Halgren, T. A. The Merck Force Field. *J. Comp. Chem.* **17,** 490–641 (1996).
32 Frisch, M. J. *et al.* Gaussian 09, Revision B.01 (Gaussian, Inc., Wallingford CT, 2009).
33 Becke, A. D. Density-functional thermochemistry. III. The role of exact exchange. *J. Chem. Phys.* **98,** 5648–5652 (1993).
34 Hariharan, P. C. & Pople, J. A. Accuracy of AH, equilibrium geometries by single determinant molecular orbital theory. *Mol. Phys.* **27,** 209–214 (1974).
35 Hariharan, P. C. & Pople, J. A. The influence of polarization functions on molecular orbital hydrogenation energies. *Theor. Chim. Acta* **28,** 213–222 (1973).
36 Francl, M. M. *et al.* Self-consistent molecular orbital methods. XXIII. A polarization-type basis set for second-row elements. *J. Chem. Phys.* **77,** 3654–3665 (1982).

37 Blaudeau, J.-P., McGrath, M. P., Curtiss, L. A. & Radom, L. Extension of Gaussian-2 (G2) theory to molecules containing third-row atoms K and Ca. *J. Chem. Phys.* **107,** 5016–5021 (1997).
38 Binning, R. C. Jr. & Curtiss, L. A. Compact contracted basis sets for third-row atoms: Ga-Kr. *J. Comput. Chem.* **11,** 1206–1216 (1990).
39 Rassolov, V. A., Ratner, M. A., Pople, J. A., Redfern, P. C. & Curtiss, L. A. 6-31G* basis set for third-row atoms. *J. Comput. Chem.* **22,** 976–984 (2001).
40 Rassolov, V. A., Pople, J. A., Ratner, M. A. & Windus, T. L. 6-31G* basis set for atoms K through Zn. *J. Chem. Phys.* **109,** 1223–1229 (1998).
41 Gordon, M. S. The isomers of silacyclopropane. *Chem. Phys. Lett.* **76,** 163–168 (1980).
42 Cances, E., Mennucci, B. & Tomasi, J. A new integral equation formalism for the polarizable continuum model: theoretical background and applications to isotropic and anisotropic dielectrics. *J. Chem. Phys.* **107,** 3032–3041 (1997).
43 Mennucci, B. & Tomasi, J. Continuum solvation models: a new approach to the problem of solutés charge distribution and cavity boundaries. *J. Chem. Phys.* **106,** 5151–5158 (1997).
44 Cossi, M., Barone, V., Mennucci, B. & Tomasi, J. *Ab-initio* study of ionic solutions by a polarizable continuum dielectric model. *Chem. Phys. Lett.* **286,** 253–260 (1998).
45 Clark, T., Chandrasekhar, J., Spitznagel, G. W. & Schleyer, P. V. R. Efficient diffuse function-augmented basis-sets for anion calculations. 3. The 3-21+G basis set for 1st-row elements, Li-F. *J. Comp. Chem.* **4,** 294–301 (1983).
46 McLean, A. D. & Chandler, G. S. Contracted Gaussian-basis sets for molecular calculations. 1. 2nd row atoms, Z=11–18. *J. Chem. Phys.* **72,** 5639–5648 (1980).
47 Raghavachari, K, Binkley, J. S., Seeger, R. & Pople, J. A. Self-consistent molecular orbital methods. 20. Basis set for correlated wave-functions. *J. Chem. Phys.* **72,** 650–654 (1980).
48 Frisch, M. J., Pople, J. A. & Binkley, J. S. Self-consistent molecular orbital methods. 25. Supplementary functions for Gaussian basis sets. *J. Chem. Phys.* **80,** 3265–3269 (1984).
49 McWeeny, R. Perturbation theory for Fock-Dirac density matrix. *Phys. Rev.* **126,** 1028–1034 (1962).
50 Ditchfield, R. Self-consistent perturbation theory of diamagnetism. 1. Gauge-invariant LCAO method for NMR chemical shifts. *Mol. Phys.* **27,** 789–807 (1974).
51 Wolinski, K., Hilton, J. F. & Pulay, P. Efficient implementation of the Gauge-independent atomic orbital method for NMR chemical shift calculations. *J. Am. Chem. Soc.* **112,** 8251–8260 (1990).
52 Deng, W., Cheeseman, J. R. & Frisch, M. J. Calculation of nuclear spin-spin coupling constants of molecules with first and second row atoms in study of basis set dependence. *J. Chem. Theory Comput.* **2,** 1028–1037 (2006).
53 Navarro-Vazquez, A., Cobas, J. C., Sardina, F. J., Casanueva, J. & Diez, E. A graphical tool for the prediction of vicinal proton-proton $^3J_{HH}$ coupling constants. *J. Chem. Inf. Comput. Sci.* **44,** 1680–1685 (2004).